Supplementary material

Title Loss of Diurnal Oscillatory Rhythms in Gut Microbiota Correlates with Progression of Atherosclerosis

Authors He Zhang[1], Xiaohan Zhang[1], Zihan Yun[1], Suhua Cang[1], Yating Shao[1], Yang Chen[1], Erteng Jia [2]*, Renjin Chen[1]*

Author affiliations

[1] School of Life Sciences, Xuzhou Medical University, 221004, Xuzhou, China

[2] Xuzhou Medical University, 221004, Xuzhou, China

Table S1 Primers used for real-time PCR analysis

Targets	Primer sequence 5′-3′	Product size
ABCA1	Forward: GCTTGTTGGCCTCAGTTAAGG Reverse: GTAGCTCAGGCGTACAGAGAT	135 bp
APOA1	Forward: GCTCAAGAGCAACCCTACCTT Reverse: GCTTTCTCGCCAAGTGTCTTC	75 bp
SR-B1	Forward: TTTGGAGTGGTAGTAAAAAGGGC Reverse: TGACATCAGGGACTCAGAGTAG	71 bp
TNFα	Forward: ATCCGCGACGTGGAACTG Reverse: ACCGCCTGGAGTTCTGGAA	70 bp
MCP1	Forward: GCTCAGCCAGATGCAGTTAAC Reverse: CTCTCTCTTGAGCTTGGTGAC	153 bp
IL-1β	Forward: GCCCATCCTCTGTGACTCAT Reverse: AGGCCACAGGTATTTTGTCG	230 bp
Il6	Forward: AGTTGCCTTCTTGGGACTGA Reverse: TCCACGATTTCCCAGAGAAC	159 bp
GADPH	Forward: AGCTTGTCATCAACGGGAAG Reverse: TTTGATGTTAGTGGGGTCTCG	62 bp
Blautia coccoides	Forward: AAATGACGGTACCTGACTAA Reverse: CTTTGAGTTTCATTCTTGCGAA	438 bp

ABCA1, ATP-binding cassette transporter A1; APOA1, apolipoprotein A-I; SR-B1, Scavenger Receptor Class B type 1; TNFα, tumor necrosis factor; MCP1, monocyte chemoattractant protein 1; IL-1β, interleukin 1 beta; Il6, Interleukin-6; GADPH, glyceraldehyde-3-phosphate dehydrogenase

Figure S1

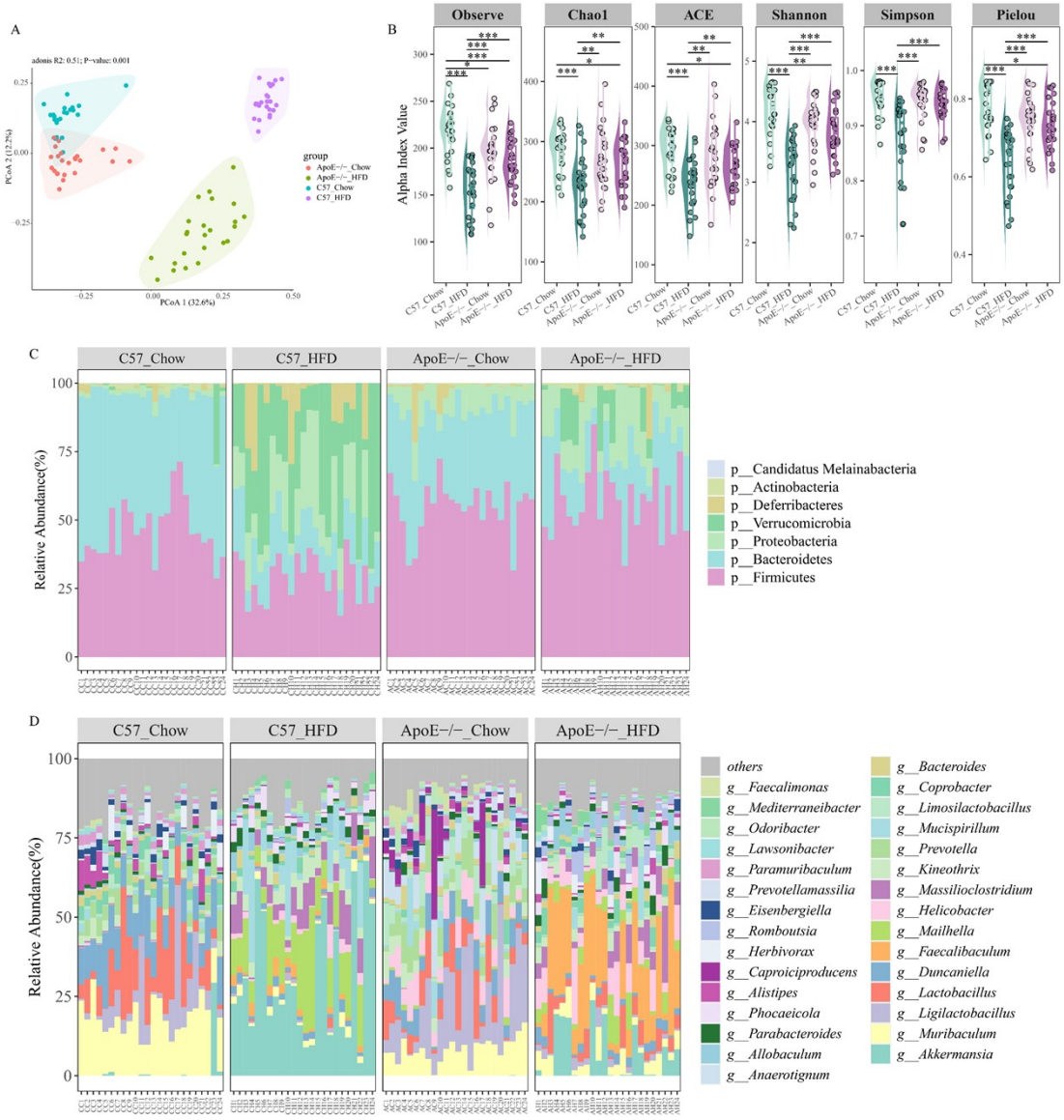

Figure S1 Fecal bacterial composition of C57_Chow, C57_HFD, *Apoe*$^{-/-}$_Chow, and *Apoe*$^{-/-}$_HFD mice under *ad libitum* conditions. (A) Principal-coordinates analysis (PCoA) of fecal microbiota among C57_Chow, C57_HFD, *Apoe*$^{-/-}$_Chow, and *Apoe*$^{-/-}$_HFD mice; PCoA was performed based on the Bray–Curtis metric. Relative variable importance (R2) and significance (*P*) were calculated by PERMANOVA (Adonis) analysis; (B) α-diversity of the fecal microbiota among C57_Chow, C57_HFD, *Apoe*$^{-/-}$_Chow and *Apoe*$^{-/-}$_HFD mice; (C) Barplot of fecal microbiota at the phylum level. Each bar represents an individual mouse and each color an individual phylum; (D) Barplot of fecal microbiota at the genus level. Each bar represents an individual mouse and each color is an individual genus. C57_Chow, C57BL/6 mice with standard diet; C57_HFD, C57BL/6 mice with high-fat, high-cholesterol diet; *Apoe*$^{-/-}$_Chow, *Apoe*$^{-/-}$ mice with standard diet; *Apoe*$^{-/-}$_HFD, *Apoe*$^{-/-}$ mice with high-fat, high-cholesterol diet. * indicates $P < 0.05$, ** indicates $P < 0.01$, *** indicates $P < 0.001$; n=24.

Figure S2

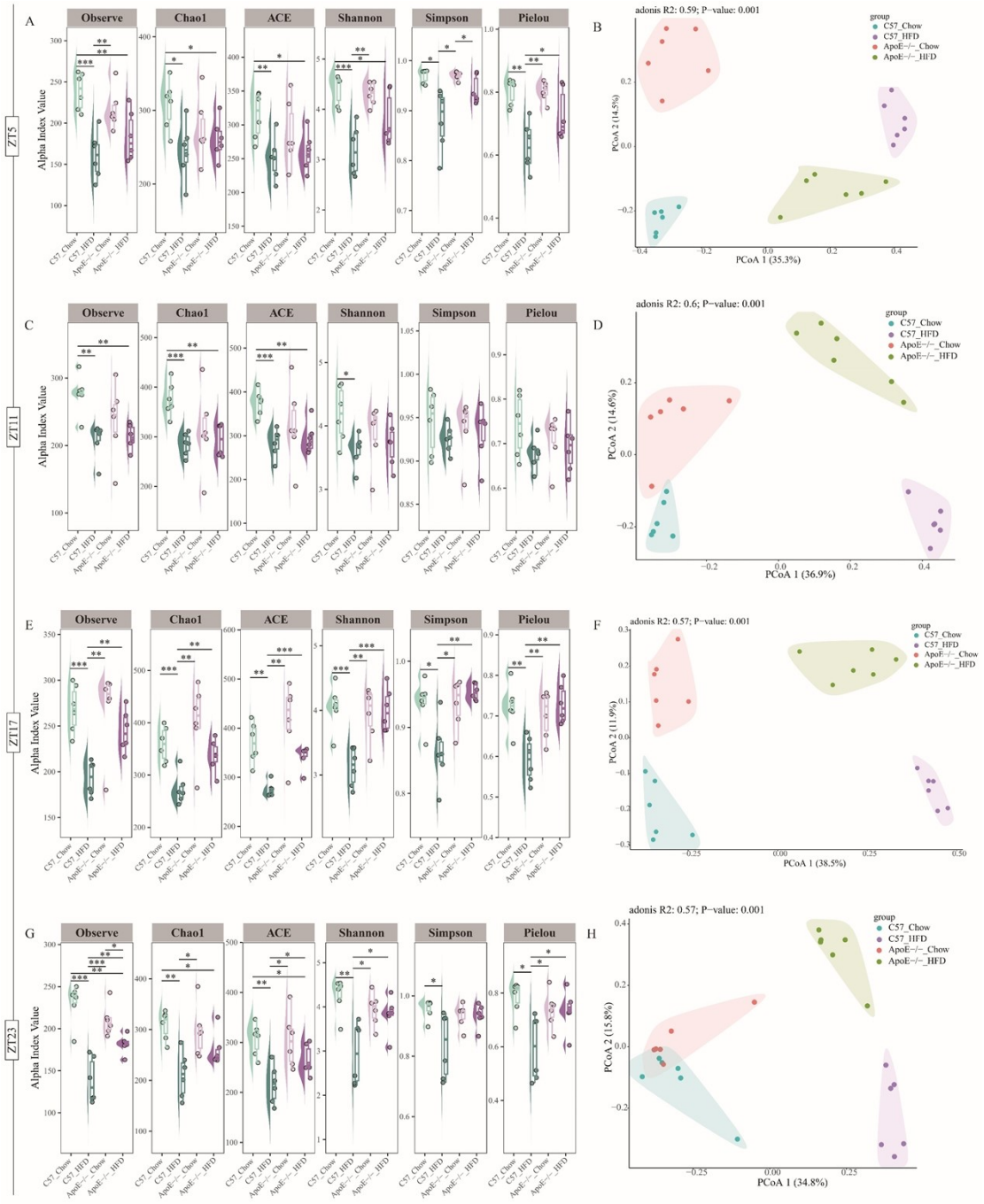

Figure S2 Composition of the fecal microbial taxa at the phylum and genus level of C57_Chow, C57_HFD, *Apoe*$^{-/-}$_Chow, and *Apoe*$^{-/-}$_HFD mice at different time points. (A, C, E, G) Barplot of fecal microbiota at the phylum at ZT5, ZT11, ZT17, and ZT23. (B, D, F, H) Barplot of fecal microbiota at the genus at ZT5, ZT11, ZT17, and ZT23. ZT, zeitgeber; * indicates $P < 0.05$, ** indicates $P < 0.01$, *** indicates $P < 0.001$; n=6.

Figure S3

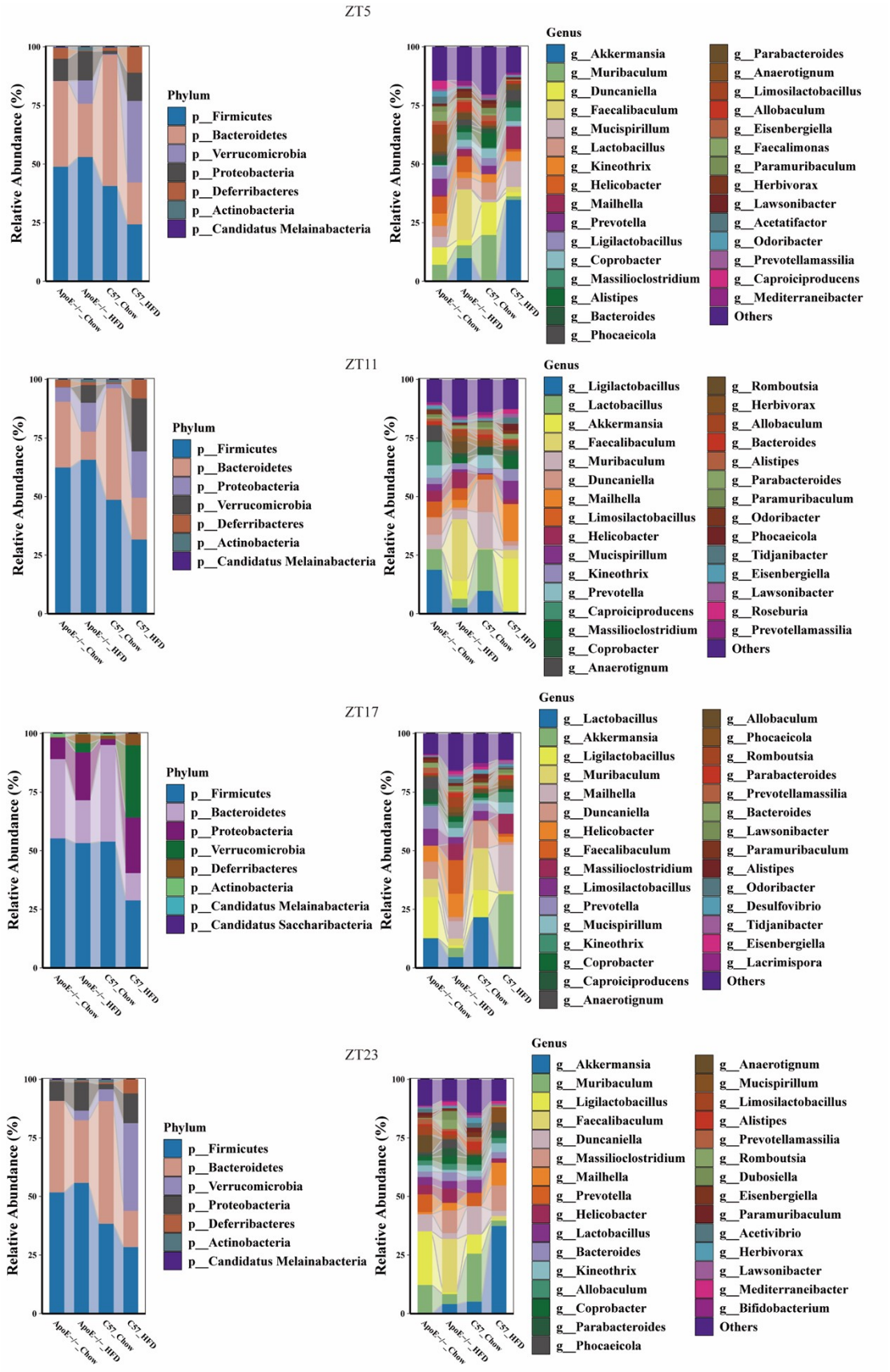

Figure S3 Dynamic change of α-diversity and β-diversity of fecal microbiota of C57_Chow,

C57_HFD, *Apoe*$^{-/-}$_Chow and *Apoe*$^{-/-}$_HFD mice. (A, C, E, G) Dynamic change in α-diversity of fecal microbiota in C57_Chow, C57_HFD, *Apoe*$^{-/-}$_Chow and *Apoe*$^{-/-}$_HFD mice; (B, D, F, H) Dynamic change in β-diversity of fecal microbiota in C57_Chow, C57_HFD, *Apoe*$^{-/-}$_Chow and *Apoe*$^{-/-}$_HFD mice; Relative variable importance (R2) and significance (*P*) were calculated by PERMANOVA (Adonis) analysis. * indicates $P < 0.05$, ** indicates $P < 0.01$; n=6.

Figure S4

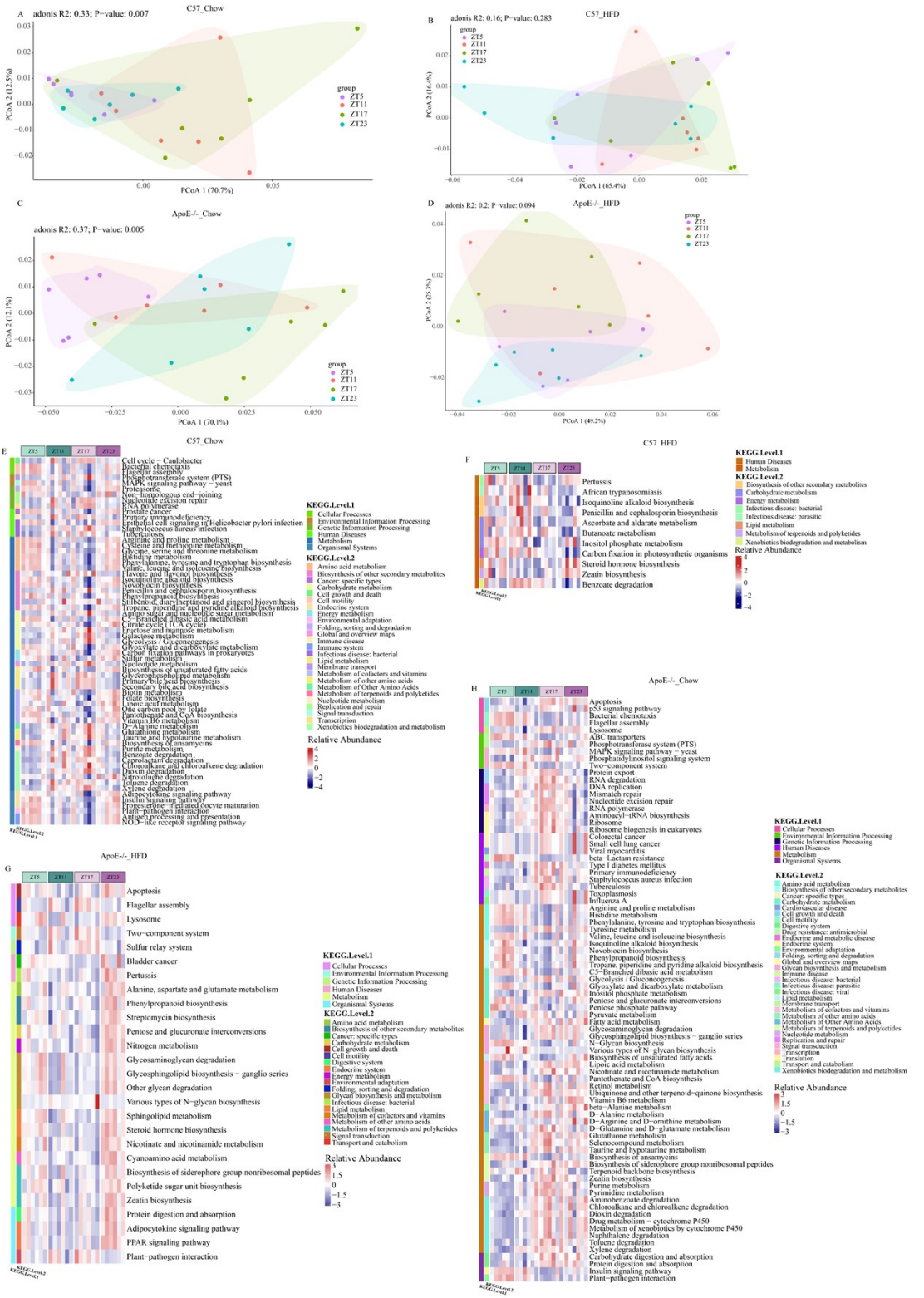

Figure S4 Daily fluctuation of microbial functions of C57_Chow, C57_HFD, *Apoe*$^{-/-}$_Chow, and *Apoe*$^{-/-}$_HFD mice. (A-D) PCoA of fecal microbial function at ZT5, ZT11, ZT17, and ZT23. Relative variable importance (R2) and significance (P) were calculated by PERMANOVA (Adonis) analysis. (E-H) Heatmap depicting the relative abundance of rhythmic KEGG level3 of fecal

microbial function C57_Chow, C57_HFD, *Apoe*$^{-/-}$_Chow, and *Apoe*$^{-/-}$_HFD, respectively. PICRUSt2 was used to predict changes in microbial functions that might be associated with changes in OTU abundance detected through 16S sequencing. The rhythmicity analysis was finished by non-parametric JTK analysis. n=6.

Figure S5

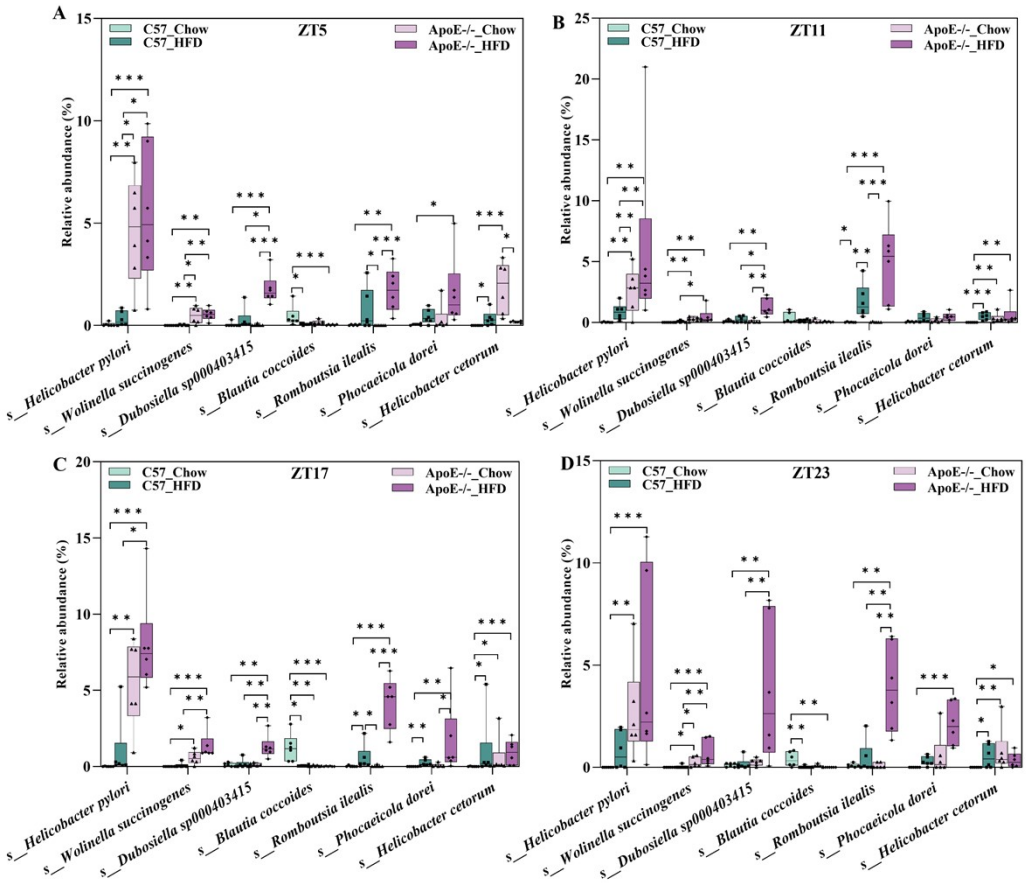

Figure S5 Differences in the relative abundance of species among four groups of mice at ZT5, ZT11, ZT17, and ZT23, respectively. Relative abundance was expressed as mean ± standard error. * indicates $P < 0.05$, ** indicates $P < 0.01$, *** indicates $P < 0.001$; n=6.

Figure S6

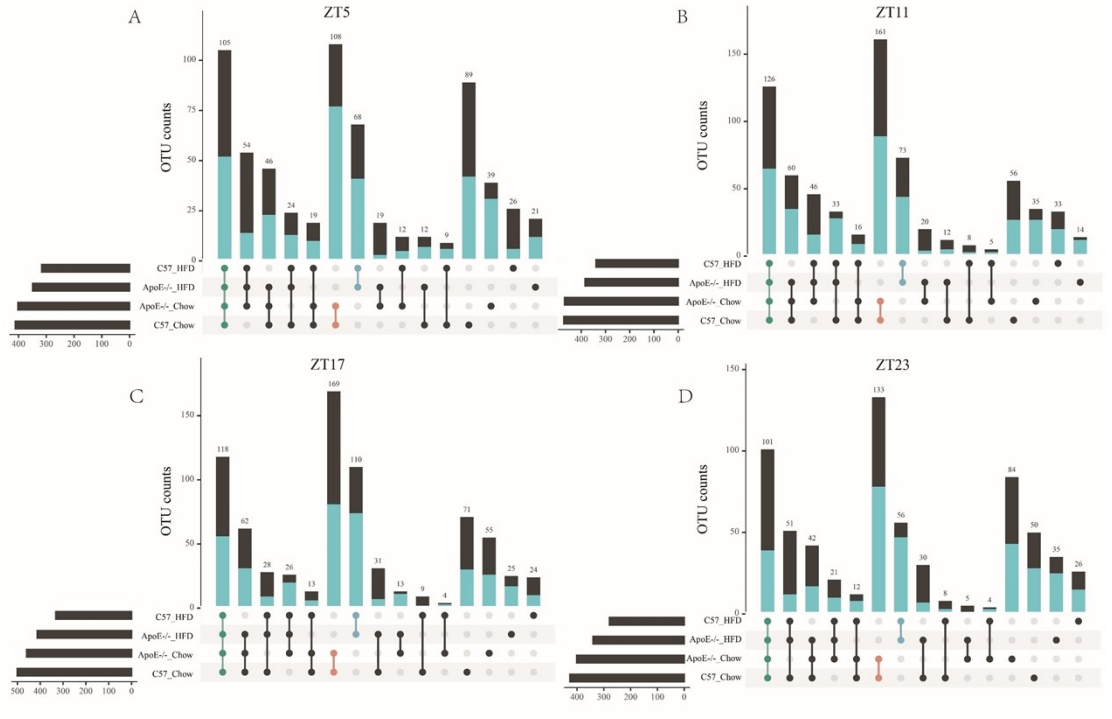

Figure S6 OTU counts of fecal microbiota in C57_Chow, C57_HFD, *Apoe*$^{-/-}$_Chow, and *Apoe*$^{-/-}$_HFD mice at different time points within a day. (A) ZT5; (B) ZT11; (C) ZT17; (D) ZT23. Filter out OTUs within the group that have an OTU count of 0 for more than half of their occurrences within the same group. The cyan columns represent OTU belonging to Firmicutes.

Figure S7

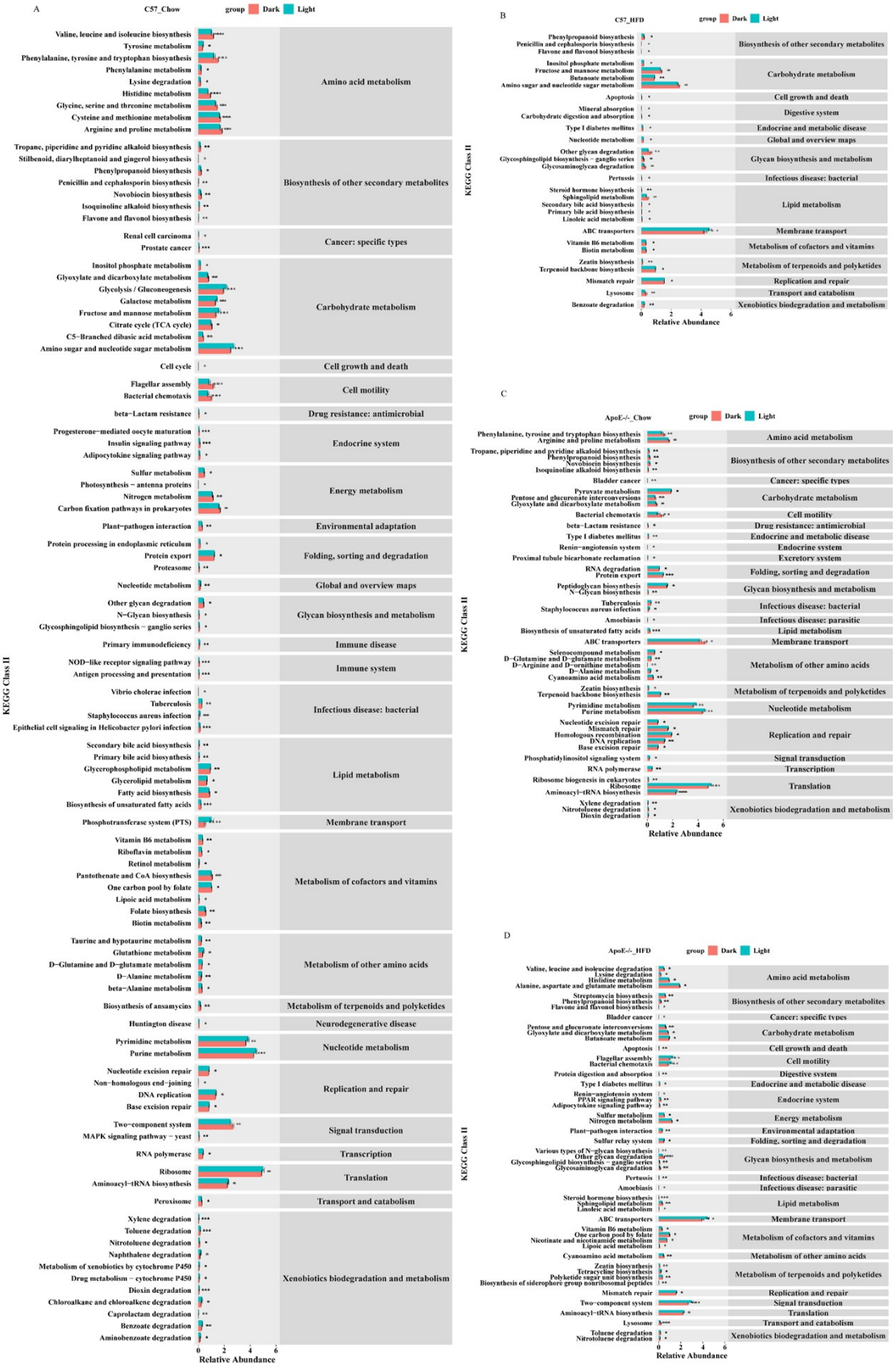

Figure S7 Daily differences in microbial functions of C57_Chow, C57_HFD, *Apoe*$^{-/-}$_Chow,

and *Apoe*$^{-/-}$_HFD mice. (A) C57_Chow mice; (B) C57_HFD mice; (C) *Apoe*$^{-/-}$_Chow mice; (D) *Apoe*$^{-/-}$_HFD mice. Relative abundance was expressed as mean ± standard error. * indicates $P < 0.05$, ** indicates $P < 0.01$, *** indicates $P < 0.001$; n=12.

Figure S8

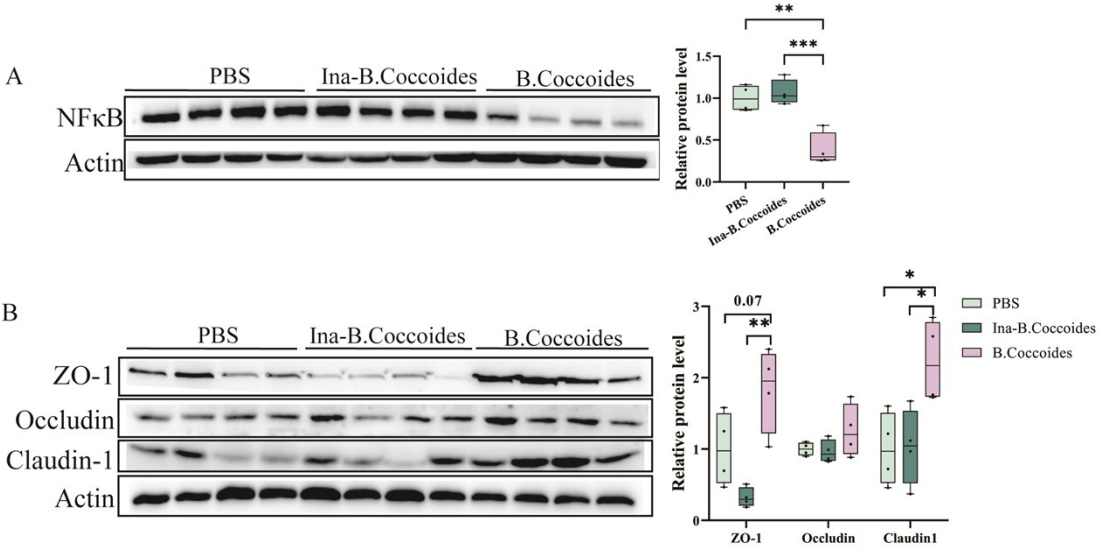

Figure S8 *B.Coccoides* intervention significantly improved the colon barrier function of *Apoe*$^{-/-}$ mice with HCHFD. (A) *B.Coccoides* intervention significantly inhibits the expression level of NF-κB; (B) *B.Coccoides* intervention significantly increased the expression levels of ZO-1 and Claudin1. Relative abundance was expressed as mean ± standard error. * indicates $P < 0.05$, ** indicates $P < 0.01$, *** indicates $P < 0.001$; n=4.